1 Scattering of light by an array of atoms

In our experiment we observe the scattering of photons from atoms confined in an optical lattice, here we treat this situation by obtaining the the field scattered from a single atom and then summing the field contributions from all the atoms coherently at the location of our detector. The main goal of this document is to find the connection between the intensity that we measure in our cameras and the spin structure factor as calculated by the theorists in our collaboration.

1.1 Electric field and intensity due to a single atom

To calculate the scattered field, one uses the source-field expression, which relates the radiated field to the emitting dipole moment, this is derived in the standard textbooks [1, 2]. The field at the position of the detector $\boldsymbol{r}_D$ is given by

$$E^{(+)}(\boldsymbol{r}_D, t) = \eta e^{-i\omega_L(t-r_D/c)} S_- \left(t - \frac{r_D}{c}\right) \tag{1}$$

where η is a proportionality factor that we will address later on. The time-averaged intensity at the detector is

$$\begin{aligned} \langle I(t)\rangle =& \langle E^{(-)}(\boldsymbol{r}_D, t) E^{(+)}(\boldsymbol{r}_D, t)\rangle \\ =& |\eta|^2 \langle S_+(t - r_D/c) S_-(t - r_D/c)\rangle \\ =& |\eta|^2 \langle S_+ S_-\rangle \\ =& |\eta|^2 \rho_{ee} \end{aligned} \tag{2}$$

In the third line the time dependence is dropped since we are interested in the steady state solution. We can write the $S_\pm$ operators of the atoms as

$$S_\pm = \langle S_\pm\rangle + \delta S_\pm \tag{3}$$

which defines the difference, δS, between $S_\pm$ and its average value. Writing $S_\pm$ this way allows us to distinguish between two components in the radiated light, the radiation of the average dipole $\langle S_\pm\rangle$ which is the radiation of a classical oscillating dipole with a phase that is well defined relative to the incident laser field, and the radiation form the $\delta S_\pm$ component which does not have a phase that is well defined relative to the incident field because it comes form the fluctuating part of the atomic dipole. The intensity is then a sum of coherent and incoherent parts

$$I = \eta^2 \langle S_+\rangle\langle S_-\rangle + \eta^2 \langle \delta S_+ \delta S_-\rangle \tag{4}$$

where we have used the fact that by definition $\langle \delta S_\pm\rangle = 0$. The first and second terms of this equation are the coherent and incoherent intensity which can be calculated by using the steady-state solutions to the optical Bloch equations:

$$\langle S_\pm\rangle = u \pm iv \tag{5}$$

$$u = \frac{\Delta}{\Gamma\sqrt{I_\mathrm{p}/I_\mathrm{sat}}} \frac{s}{1+s} \tag{6}$$

$$v = \frac{1}{2\sqrt{I_\mathrm{p}/I_\mathrm{sat}}} \frac{s}{1+s} \tag{7}$$

$$\tag{8}$$

where s is the saturation parameter for an incident probe with intensity $I_{\rm p}$:

$$s = \frac{2I_{\rm p}/I_{\rm sat}}{1+4(\Delta/\Gamma)^2} = \frac{s_0}{1+4(\Delta/\Gamma)^2} \tag{9}$$

and we have defined $s_0 = 2I_{\rm p}/I_{\rm sat}$. The coherent and incoherent intensities are

$$\begin{aligned} \frac{1}{\eta^2} I_{\rm coh} =& \frac{1}{2}\frac{s}{(1+s)^2} = \rho_{ee}\frac{1}{1+s} \\ \frac{1}{\eta^2} I_{\rm incoh} =& \langle S_+ S_-\rangle - \langle S_+\rangle\langle S_-\rangle = \frac{1}{2}\frac{s^2}{(1+s)^2} = \rho_{ee}\frac{s}{1+s} \end{aligned} \tag{10}$$

Note that if we add up coherent and incoherent part we get the familiar result $I = \eta^2\rho_{ee}$, where the total intensity is simply proportional to the population of the excited state.

1.2 Scattering cross-section

Now we will turn onto the evaluation of η, the proportionality factor between the field and the emitting dipole. Knowledge of η will allow us to sum coherently the field from a collection of atoms.

We start by considering the transition matrix element between the following initial and final states of the atom+photon system:

$$\begin{aligned} |\varphi_i\rangle =& |g; \boldsymbol{k}\boldsymbol{\varepsilon}\rangle \\ |\varphi_f\rangle =& |g'; \boldsymbol{k}'\boldsymbol{\varepsilon}'\rangle \end{aligned} \tag{11}$$

These states represent the absorption and re-emission of a single photon by the atom, with two possibly different initial and final photon states, and two possibly different initial and final atom ground states.

The transition rate to from $i \to f$ is given by

$$w_{fi} = \frac{2\pi}{\hbar}|\mathcal{T}_{fi}|^2\delta(E_f - E_i) \tag{12}$$

Where we use the notation in [2] (see Exercise 5 on pg. 530), and $\mathcal{T}_{fi}$ is given by

$$\mathcal{T}_{fi} = \frac{\langle g; \boldsymbol{k}'\boldsymbol{\varepsilon}'|H_I'|e;0\rangle\langle e;0|H_I'|g;\boldsymbol{k}\boldsymbol{\varepsilon}\rangle}{\hbar\omega - \hbar\omega_0 + i\hbar(\Gamma/2)} \tag{13}$$

where H_I' is the interaction Hamiltonian

$$H_I' = -\boldsymbol{d}\cdot\boldsymbol{E}_\perp(\boldsymbol{r}) \tag{14}$$

and[1]

$$\boldsymbol{E}_\perp(\boldsymbol{r}) = i\sum_j \left[\frac{\hbar\omega_j}{2\varepsilon_0 L^3}\right]^{1/2}\left(\hat{a}_j\boldsymbol{\varepsilon}_j e^{i\boldsymbol{k}_j\cdot\boldsymbol{r}} - \hat{a}_j^+\boldsymbol{\varepsilon}_j^* e^{-i\boldsymbol{k}_j\cdot\boldsymbol{r}}\right) \tag{15}$$

Notice that there is an intermediate excited state $|e;0\rangle$, since the absorption-emission event is a second order process.

[1] Notice that the presence of ϵ_0 reveals that we are using SI units, following the treatment in [2].

Using the expressions for H_I' and $\boldsymbol{E}_\perp(\boldsymbol{r})$ we obtain for the matrix element

$$\langle e;0|H_I'|g;\boldsymbol{k}\boldsymbol{\varepsilon}\rangle = -i\sqrt{\frac{\hbar\omega}{2\varepsilon_0 L^3}}\langle e|(\boldsymbol{d}\cdot\boldsymbol{\varepsilon}^*)e^{-i\boldsymbol{k}\cdot\boldsymbol{r}}|g\rangle \tag{16}$$

At this point the textbook treatment usually assumes that the atom is at the origin and that the size of the atom wavefunction is very small compared to $|\boldsymbol{k}|^{-1}$, and so the exponential inside the matrix element typically does not show up. In our case the atom is in a lattice site and its center of mass state is one of the harmonic oscillator states of a lattice well, which is large enough that the exponential term cannot be neglected.

The states $|e\rangle$ and $|g\rangle$ include the center of mass and internal states of the atom. We separate the center of mass part, and keep the labels e, g for the internal states. Also, we denote the center of mass initial and final states as $|u\rangle$ and $|u'\rangle$ respectively, and the center of mass state of the intermediate excited state as $|v\rangle$, we have

$$\langle e;0|H_I'|g;\boldsymbol{k}\boldsymbol{\varepsilon}\rangle = -i\sqrt{\frac{\hbar\omega}{2\varepsilon_0 L^3}}\langle e|\boldsymbol{d}\cdot\boldsymbol{\varepsilon}^*|g\rangle\langle v|e^{-i\boldsymbol{k}\cdot\boldsymbol{r}}|u\rangle \tag{17}$$

and similarly

$$\langle g;\boldsymbol{k}'\boldsymbol{\varepsilon}'|H_I'|e;0\rangle = i\sqrt{\frac{\hbar\omega'}{2\varepsilon_0 L^3}}\langle g|\boldsymbol{d}\cdot\boldsymbol{\varepsilon}'|e\rangle\langle u'|e^{i\boldsymbol{k}'\cdot\boldsymbol{r}}|v\rangle \tag{18}$$

This gives for the matrix element

$$\mathcal{T}_{fi} = \sum_v \frac{\sqrt{\omega\omega'}}{2\varepsilon_0 L^3}\frac{\langle g|\boldsymbol{d}\cdot\boldsymbol{\varepsilon}'|e\rangle\langle e|\boldsymbol{d}\cdot\boldsymbol{\varepsilon}^*|g\rangle\langle u'|e^{i\boldsymbol{k}'\cdot\boldsymbol{r}}|v\rangle\langle v|e^{-i\boldsymbol{k}\cdot\boldsymbol{r}}|u\rangle}{\omega-\omega_0+i(\Gamma/2)} \tag{19}$$

where we have summed over all possible intermediate center of mass states. Note that the sum can be taken out using the closure relation $\sum_v |v\rangle\langle v| = \mathbb{1}$.

In our experiment we are driving a sigma-minus transition so we can consider only the projection of $\boldsymbol{d}$ onto $\boldsymbol{\varepsilon}_-$

$$\langle e|\boldsymbol{d}\cdot\boldsymbol{\varepsilon}^*|g\rangle \equiv d_-(\boldsymbol{\varepsilon}_-\cdot\boldsymbol{\varepsilon}^*) \tag{20}$$

which leads to

$$\mathcal{T}_{fi} = \frac{\sqrt{\omega\omega'}}{2\varepsilon_0 L^3}\frac{|d_-|^2(\boldsymbol{\varepsilon}_+\cdot\boldsymbol{\varepsilon}')(\boldsymbol{\varepsilon}^*\cdot\boldsymbol{\varepsilon}_-)}{\omega-\omega_0+i(\Gamma/2)}\langle u'|e^{i(\boldsymbol{k}'-\boldsymbol{k})\cdot\boldsymbol{r}}|u\rangle \tag{21}$$

We use the relation between $|d_-|^2$ and the linewidth of the transition

$$|d_-|^2 = 3\pi\varepsilon_0\hbar\left(\frac{c}{\omega_0}\right)^3\Gamma \tag{22}$$

and also the approximation $\omega' \approx \omega \approx \omega_0$ for the square root in the denominator to obtain

$$\mathcal{T}_{fi} = \frac{3}{k^2}\frac{\pi\hbar c}{L^3}(\boldsymbol{\varepsilon}_+\cdot\boldsymbol{\varepsilon}')(\boldsymbol{\varepsilon}^*\cdot\boldsymbol{\varepsilon}_-)\frac{\Gamma/2}{\omega-\omega_0+i(\Gamma/2)}\langle u'|e^{i(\boldsymbol{k}'-\boldsymbol{k})\cdot\boldsymbol{r}}|u\rangle \tag{23}$$

To obtain the scattering rate of photons towards a certain solid angle Ω', we must sum over all values of k' in the direction of Ω'. The number of final states with energy between $\hbar ck'$ and $\hbar c(k'+\mathrm{d}k')$ whose wave vector points inside the solid angle $\mathrm{d}\Omega'$ is given by

$$\rho(\hbar ck')\hbar c\mathrm{d}k'\mathrm{d}\Omega' = \frac{L^3}{8\pi^3}k'^2\mathrm{d}k'\mathrm{d}\Omega' \tag{24}$$

where ρ is the density of states, which is a function of the photon energy $\hbar ck$. We use the density of states to replace the sum over k' with an integral, and obtain the total transition rate in the direction Ω':

$$\begin{aligned}\sum_f w_{fi} =& \frac{2\pi}{\hbar}\mathrm{d}\Omega' \int_0^\infty \frac{k'^2 \mathrm{d}k'}{(2\pi/L^3)^3}|\mathcal{T}_{fi}|^2\delta(\hbar ck' - \hbar ck) \\ =& \mathrm{d}\Omega' \frac{9}{4k^2}\frac{c}{L^3}|(\boldsymbol{\varepsilon}_+\cdot\boldsymbol{\varepsilon}')(\boldsymbol{\varepsilon}^*\cdot\boldsymbol{\varepsilon}_-)|^2 \left|\frac{\Gamma/2}{\omega-\omega_0+i(\Gamma/2)}\langle u'|e^{i(\boldsymbol{k}'-\boldsymbol{k})\cdot\boldsymbol{r}}|u\rangle\right|^2 \\ =& \mathrm{d}\Omega' \frac{9}{4k^2}\frac{c}{L^3}|(\boldsymbol{\varepsilon}_+\cdot\boldsymbol{\varepsilon}')(\boldsymbol{\varepsilon}^*\cdot\boldsymbol{\varepsilon}_-)|^2 \frac{(\Gamma/2)^2}{\Delta^2+(\Gamma/2)^2}\left|\langle u'|e^{i(\boldsymbol{k}'-\boldsymbol{k})\cdot\boldsymbol{r}}|u\rangle\right|^2\end{aligned} \tag{25}$$

If we consider the flux corresponding to the state of the initial photon $\phi = c/L^3$ then we can define the differential cross section

$$\frac{\mathrm{d}\sigma}{\mathrm{d}\Omega'} = \frac{\sum_f w_{fi}}{\mathrm{d}\Omega'\phi} = \frac{9}{4k^2}|(\boldsymbol{\varepsilon}_+\cdot\boldsymbol{\varepsilon}')(\boldsymbol{\varepsilon}^*\cdot\boldsymbol{\varepsilon}_-)|^2 \frac{(\Gamma/2)^2}{\Delta^2+(\Gamma/2)^2}\left|\langle u'|e^{i(\boldsymbol{k}'-\boldsymbol{k})\cdot\boldsymbol{r}}|u\rangle\right|^2 \tag{26}$$

From here we can write down the intensity on a detector located at $\boldsymbol{r}_D$ in the direction of $\mathrm{d}\Omega'$ as [2]

$$\begin{aligned}I =& \frac{1}{r_D^2}\frac{\mathrm{d}\sigma}{\mathrm{d}\Omega'}I_\mathrm{p} = \frac{1}{r_D^2}\frac{\mathrm{d}\sigma}{\mathrm{d}\Omega'}\frac{\hbar ck^3\Gamma}{6\pi}\frac{I_\mathrm{p}}{I_\mathrm{sat}} \\ =& \frac{\hbar ck\Gamma}{r_D^2}\frac{9}{4(6\pi)}|(\boldsymbol{\varepsilon}_+\cdot\boldsymbol{\varepsilon}')(\boldsymbol{\varepsilon}^*\cdot\boldsymbol{\varepsilon}_-)|^2\left|\langle u'|e^{i(\boldsymbol{k}'-\boldsymbol{k})\cdot\boldsymbol{r}}|u\rangle\right|^2 \frac{s_0/2}{4(\Delta/\Gamma)^2+1}\end{aligned} \tag{27}$$

We identify the last fraction in this product as ρ_{ee} (in the limit of low intensity). Comparing with Eq. 10 we can write down an expression for η,

$$\eta = \left[\frac{\hbar ck\Gamma}{r_D^2}\frac{9}{24\pi}\right]^{1/2}(\boldsymbol{\varepsilon}_+\cdot\boldsymbol{\varepsilon}')(\boldsymbol{\varepsilon}^*\cdot\boldsymbol{\varepsilon}_-)\langle u'|e^{i(\boldsymbol{k}'-\boldsymbol{k})\cdot\boldsymbol{r}}|u\rangle \tag{28}$$

With an exact expression for η we can obtain the field radiated by each atom and proceed to sum the field coherently for a collection of atoms.

1.3 Summation for a collection of atoms

For a collection of atoms, the resulting field is the sum of the field produced by each individual atom, so we have

$$\langle I(t)\rangle = \left\langle \left(\sum_m E_m^{(-)}(\boldsymbol{r}_D,t)\right)\left(\sum_n E_n^{(+)}(\boldsymbol{r}_D,t)\right)\right\rangle \tag{29}$$

where we have labeled the atoms with the indices m and n. We insert the source-field expression from Eq. 1 (dropping the time dependence)

$$I = \sum_{mn}\eta_m\eta_n^*\langle S_{m+}S_{n-}\rangle \tag{30}$$

[2] Later on we will sum over output polarizations and final center of mass states of the atom, since our detection is insensitive to them.

Using $S = \langle S\rangle + \delta S$, as we did above to obtain the coherent and incoherent parts of the intensity, we obtain

$$\begin{aligned} I &= \sum_{mn} \eta_m \eta_n^* \left(\langle S_{m+}\rangle \langle S_{n-}\rangle + \langle \delta S_{m+} \delta S_{n-}\rangle \right) \\ &= \sum_{mn} \eta_m \eta_n^* \langle S_{m+}\rangle \langle S_{n-}\rangle + \sum_n |\eta_n|^2 \langle \delta S_{n+} \delta S_{n-}\rangle \end{aligned} \tag{31}$$

The steady state solutions of the optical Bloch equations are used again to evaluate the expectation values and we obtain for I

$$\begin{aligned} I = \sum_{mn} \eta_m \eta_n^* \left(\frac{\Delta_m}{\Gamma\sqrt{I_\mathrm{p}/I_\mathrm{sat}}} \frac{s_m}{1+s_m} + i \frac{1}{2\sqrt{I_\mathrm{p}/I_\mathrm{sat}}} \frac{s_m}{1+s_m} \right) \left(\frac{\Delta_n}{\Gamma\sqrt{I_\mathrm{p}/I_\mathrm{sat}}} \frac{s_n}{1+s_n} - i \frac{1}{2\sqrt{I_\mathrm{p}/I_\mathrm{sat}}} \frac{s_n}{1+s_n} \right) \\ + \sum_n |\eta_n|^2 \frac{1}{2} \frac{s_n^2}{(1+s_n)^2} \end{aligned} \tag{32}$$

$$I = \sum_{mn} \eta_m \eta_n^* \frac{s_m s_n}{(I_\mathrm{p}/I_\mathrm{sat})(1+s_m)(1+s_n)} \left(\frac{\Delta_m \Delta_n}{\Gamma^2} + i\frac{\Delta_n}{2\Gamma} - i\frac{\Delta_m}{2\Gamma} + \frac{1}{4} \right) + \sum_n |\eta_n|^2 \frac{1}{2} \frac{s_n^2}{(1+s_n)^2} \tag{33}$$

The last term here is the incoherently scattered part due to the fluctuating fraction $\delta S_\pm$ of the atomic dipole. The cross terms do not appear in this sum because $\langle \delta S_{m+} \delta S_{n-}\rangle = 0$ for $m \neq n$; this is why this part is identified as the incoherent scattering.

We proceed to split up the first sum into same-atom ($n = m$) and different atom ($n < m$) parts

$$\begin{aligned} I = \sum_{m<n} \frac{s_m s_n}{(I_\mathrm{p}/I_\mathrm{sat})(1+s_m)(1+s_n)} \Bigg(\eta_m \eta_n^* \left(\frac{\Delta_m \Delta_n}{\Gamma^2} + i\frac{\Delta_n}{2\Gamma} - i\frac{\Delta_m}{2\Gamma} + \frac{1}{4} \right) \\ + \eta_n \eta_m^* \left(\frac{\Delta_n \Delta_m}{\Gamma^2} + i\frac{\Delta_m}{2\Gamma} - i\frac{\Delta_n}{2\Gamma} + \frac{1}{4} \right) \Bigg) \\ + \sum_n |\eta_n|^2 \frac{s_n s_n}{(I_\mathrm{p}/I_\mathrm{sat})(1+s_n)(1+s_n)} \left(\frac{\Delta_n \Delta_n}{\Gamma^2} + \frac{1}{4} \right) \\ + \sum_n |\eta_n|^2 \frac{1}{2} \frac{s_n^2}{(1+s_n)^2} \end{aligned} \tag{34}$$

$$\begin{aligned} I = \sum_{m<n} \frac{s_m s_n}{(I/I_\mathrm{sat})(1+s_m)(1+s_n)} 2\Re \left[\eta_m \eta_n^* \left(\frac{\Delta_m \Delta_n}{\Gamma^2} + i\frac{\Delta_n}{2\Gamma} - i\frac{\Delta_m}{2\Gamma} + \frac{1}{4} \right) \right] \\ + \sum_n |\eta_n|^2 \frac{1}{2} \frac{s_n}{(1+s_n)^2} + \sum_n |\eta_n|^2 \frac{1}{2} \frac{s_n^2}{(1+s_n)^2} \end{aligned} \tag{35}$$

With this expression in hand we focus our attention on the terms $\eta_m \eta_n^*$ and $|\eta_n|^2$. We start with the latter

$$|\eta_n|^2 = \frac{\hbar c k \Gamma}{r_D^2} \frac{9}{24\pi} |(\boldsymbol{\varepsilon}_+ \cdot \boldsymbol{\varepsilon}')(\boldsymbol{\varepsilon}^* \cdot \boldsymbol{\varepsilon}_-)|^2 \langle u| e^{-i(\boldsymbol{k}'-\boldsymbol{k})\cdot \boldsymbol{r}_n} |u'\rangle \langle u'| e^{i(\boldsymbol{k}'-\boldsymbol{k})\cdot \boldsymbol{r}_n} |u\rangle \tag{36}$$

and notice that we have to sum over output polarizations $\boldsymbol{\varepsilon}'$ and final center of mass states u', since our

detector does not care about either. We obtain

$$\begin{aligned}\sum_{\boldsymbol{\varepsilon}' u'} |\eta_n|^2 =& \sum_{u'} \frac{\hbar c k \Gamma}{r_D^2} \frac{9}{24\pi} \sum_{\boldsymbol{\varepsilon}'} |(\boldsymbol{\varepsilon}_+ \cdot \boldsymbol{\varepsilon}')(\boldsymbol{\varepsilon}^* \cdot \boldsymbol{\varepsilon}_-)|^2 \langle u | e^{-i(\boldsymbol{k}'-\boldsymbol{k})\cdot \boldsymbol{r}_n} | u' \rangle \langle u' | e^{i(\boldsymbol{k}'-\boldsymbol{k})\cdot \boldsymbol{r}_n} | u \rangle \\ =& \frac{\hbar c k \Gamma}{r_D^2} \frac{9}{24\pi} \Lambda \langle u | e^{-i(\boldsymbol{k}'-\boldsymbol{k})\cdot \boldsymbol{r}_n} e^{i(\boldsymbol{k}'-\boldsymbol{k})\cdot \boldsymbol{r}_n} | u \rangle \\ =& \frac{\hbar c k \Gamma}{r_D^2} \frac{9}{24\pi} \Lambda \end{aligned} \tag{37}$$

where we have used the closure relation $\sum u' |u'\rangle\langle u'| = \mathbb{1}$, and have defined for brevity

$$\Lambda = \sum_{\boldsymbol{\varepsilon}'} |(\boldsymbol{\varepsilon}_+ \cdot \boldsymbol{\varepsilon}')(\boldsymbol{\varepsilon} \cdot \boldsymbol{\varepsilon}_-)|^2 \tag{38}$$

Similarly, for $\eta_m \eta_n^*$

$$\sum_{\boldsymbol{\varepsilon}' u'_m u'_n} \eta_m \eta_n^* = \frac{\hbar c k \Gamma}{r_D^2} \frac{9}{24\pi} \Lambda \sum_{u'_m u'_n} \langle u_n | e^{-i(\boldsymbol{k}'-\boldsymbol{k})\cdot \boldsymbol{r}_n} | u'_n \rangle \langle u'_m | e^{i(\boldsymbol{k}'-\boldsymbol{k})\cdot \boldsymbol{r}_m} | u_m \rangle \tag{39}$$

In this case we cannot use the closure relation because n, m refer to different atoms. We simplify the treatment by considering only final center of mass states that are the same as the initial state: $u' = u$. In a deep lattice the number of scattering events in which the atom does not return to its original center of mass state are suppressed by a factor equal to the square of the Lamb-Dicke parameter:

$$\eta_{LD}^2 = \frac{E_R}{\hbar \omega_{\text{lattice}}} = \frac{1}{2\sqrt{V_0/E_R}} \tag{40}$$

In our experiment we use a lattice depth $V_0 = 50 E_R$ for the scattering measurement, so we have $\eta_{LD}^2 = 0.07$. This means that one in every about 14 scatters will take the atom to a different center of mass state. As long as we keep the number of photons scattered small enough we can consider only $u'_m = u_m$ and $u'_n = u_n$ in Eq. 39. The center of mass state of the atoms is the ground state of the single lattice site harmonic oscillator. This leaves us with

$$\sum_{\boldsymbol{\varepsilon}'} \eta_m \eta_n^* = \frac{\hbar c k \Gamma}{r_D^2} \frac{9}{24\pi} \Lambda \langle 0_n | e^{-i(\boldsymbol{k}'-\boldsymbol{k})\cdot \boldsymbol{r}_n} | 0_n \rangle \langle 0_m | e^{i(\boldsymbol{k}'-\boldsymbol{k})\cdot \boldsymbol{r}_m} | 0_m \rangle \tag{41}$$

1.3.1 Debye-Waller factor

For each center of mass expectation value we perform a translation $\boldsymbol{R}_n$ of the coordinate system such that the position of the n^{th} atom has a zero expectation value $\langle \boldsymbol{r}_n \rangle = 0$. A phase factor comes out that depends on the position $\boldsymbol{R}_n$ of the lattice site in which the atom is located:

$$\langle 0_n | e^{-i(\boldsymbol{k}'-\boldsymbol{k})\cdot \boldsymbol{r}_n} | 0_n \rangle = e^{-i(\boldsymbol{k}'-\boldsymbol{k})\cdot \boldsymbol{R}_n} \langle 0_n | e^{-i(\boldsymbol{k}'-\boldsymbol{k})\cdot \boldsymbol{r}_n} | 0_n \rangle \tag{42}$$

We then use the equality $\langle e^{\hat{A}}\rangle = e^{\frac{1}{2}\langle \hat{A}^2\rangle}$, which is valid for a simple harmonic oscillator, where $\hat{A}$ is any linear combination of displacement and momentum operators of the oscillator. This leaves us with

$$\begin{aligned}\langle 0_n|e^{-i(\boldsymbol{k}'-\boldsymbol{k})\cdot\boldsymbol{r}_n}|0_n\rangle =& e^{-i(\boldsymbol{k}'-\boldsymbol{k})\cdot\boldsymbol{R}_n}e^{-\frac{1}{2}\left\langle[(\boldsymbol{k}'-\boldsymbol{k})\cdot\boldsymbol{r}_n]^2\right\rangle}\\ =& e^{-i\boldsymbol{Q}\cdot\boldsymbol{R}_n}e^{-\frac{1}{2}\left\langle[\boldsymbol{Q}\cdot\boldsymbol{r}_n]^2\right\rangle}\\ =& e^{-i\boldsymbol{Q}\cdot\boldsymbol{R}_n}\prod_{i=x,y,z}e^{-\frac{1}{2}Q_i^2\langle r_{ni}^2\rangle}\\ =& e^{-i\boldsymbol{Q}\cdot\boldsymbol{R}_n}e^{-W}\end{aligned} \tag{43}$$

where we have defined the momentum transfer $\boldsymbol{Q} = \boldsymbol{k}' - \boldsymbol{k}$, and the Debye-Waller factor e^{-2W}.

Putting this back in the expression for $\eta_m\eta_n^*$ we get

$$\sum_{\boldsymbol{\varepsilon}'}\eta_m\eta_n^* = \frac{\hbar ck\Gamma}{r_D^2}\frac{9}{24\pi}\Lambda e^{i\boldsymbol{Q}(\boldsymbol{R}_m-\boldsymbol{R}_n)}e^{-2W} \tag{44}$$

And if we now return to the expression for the intensity at the detector we have

$$\begin{aligned}I = \sum_{m<n}\frac{s_m s_n}{(I_\mathrm{p}/I_\mathrm{sat})(1+s_m)(1+s_n)}2\Re\left[\frac{\hbar ck\Gamma}{r_D^2}\frac{9}{24\pi}\Lambda e^{i\boldsymbol{Q}(\boldsymbol{R}_m-\boldsymbol{R}_n)}e^{-2W}\left(\frac{\Delta_m\Delta_n}{\Gamma^2}+i\frac{\Delta_n}{2\Gamma}-i\frac{\Delta_m}{2\Gamma}+\frac{1}{4}\right)\right]\\ +\sum_n\frac{1}{2}\frac{\hbar ck\Gamma}{r_D^2}\frac{9}{24\pi}\Lambda\frac{s_n}{1+s_n}\end{aligned} \tag{45}$$

$$\begin{aligned}I =& \left(\frac{\hbar ck\Gamma}{r_D^2}\frac{9}{24\pi}\Lambda\right)\times\\ &\sum_{m<n}\frac{s_m s_n}{(I_\mathrm{p}/I_\mathrm{sat})(1+s_m)(1+s_n)}2\Re\left[e^{i\boldsymbol{Q}(\boldsymbol{R}_m-\boldsymbol{R}_n)}e^{-2W}\left(\frac{\Delta_m\Delta_n}{\Gamma^2}+i\frac{\Delta_n}{2\Gamma}-i\frac{\Delta_m}{2\Gamma}+\frac{1}{4}\right)\right]+\sum_n\frac{1}{2}\frac{s_n}{1+s_n}\end{aligned} \tag{46}$$

For a large time-of-flight, where the Debye-Waller factor goes to zero due to large extent of the expanding atom wavefunctions, this formula reduces to the the standard uncorrelated scattering for N atoms, $I \propto N\rho_{ee}$ with $\rho_{ee} = \frac{1}{2}\frac{s}{1+s}$. We can evaluate the total photon scattering rate $\Gamma_\mathrm{scatt} = \frac{1}{\hbar ck}\int Ir_D^2\mathrm{d}\Omega$, for which we use $\int\Lambda\mathrm{d}\Omega = \frac{8\pi}{3}$ and obtain

$$\Gamma_\mathrm{scatt} = \Gamma\frac{N}{2}\frac{s}{1+s} = N\Gamma\rho_{ee} \tag{47}$$

This result gives a consistency check on the prefactors that appear in Eq. 46.

1.4 Large detuning limit

We start from Eq. (46) and concentrate on the two sums, the first of which is

$$\frac{e^{-2W}}{2I_\mathrm{p}/I_\mathrm{sat}}\Re\sum_{m<n}e^{i\boldsymbol{Q}(\boldsymbol{R}_m-\boldsymbol{R}_n)}\frac{s_m s_n}{(1+s_m)(1+s_n)}\left(4\Delta_m\Delta_n+2i\Delta_n-2i\Delta_m+1\right) \tag{48}$$

where for simplicity we have now written the detunings in units of Γ. We will split this up further into four terms

$$\frac{e^{-2W}}{2I_{\rm p}/I_{\rm sat}}\Re\sum_{m<n}e^{i\boldsymbol{Q}(\boldsymbol{R}_m-\boldsymbol{R}_n)}\frac{s_m s_n}{(1+s_m)(1+s_n)}4\Delta_m\Delta_n \tag{49}$$

$$\frac{e^{-2W}}{2I_{\rm p}/I_{\rm sat}}\Re\sum_{m<n}e^{i\boldsymbol{Q}(\boldsymbol{R}_m-\boldsymbol{R}_n)}\frac{s_m s_n}{(1+s_m)(1+s_n)}2i\Delta_n \tag{50}$$

$$-\frac{e^{-2W}}{2I_{\rm p}/I_{\rm sat}}\Re\sum_{m<n}e^{i\boldsymbol{Q}(\boldsymbol{R}_m-\boldsymbol{R}_n)}\frac{s_m s_n}{(1+s_m)(1+s_n)}2i\Delta_m \tag{51}$$

$$\frac{e^{-2W}}{2I_{\rm p}/I_{\rm sat}}\Re\sum_{m<n}e^{i\boldsymbol{Q}(\boldsymbol{R}_m-\boldsymbol{R}_n)}\frac{s_m s_n}{(1+s_m)(1+s_n)} \tag{52}$$

For a detuning such that $4\Delta_m^2, 4\Delta_n^2 \gg 1$ we have

$$\frac{s}{1+s}\approx\frac{2I_{\rm p}/I_{\rm sat}}{4\Delta^2+2I_{\rm p}/I_{\rm sat}} \tag{53}$$

and the four terms above go respectively to

$$e^{-2W}2(I_{\rm p}/I_{\rm sat})\Re\sum_{m<n}e^{i\boldsymbol{Q}(\boldsymbol{R}_m-\boldsymbol{R}_n)}\frac{4\Delta_m\Delta_n}{(4\Delta_m^2+2I_{\rm p}/I_{\rm sat})(4\Delta_n^2+2I_{\rm p}/I_{\rm sat})} \tag{54}$$

$$e^{-2W}2(I_{\rm p}/I_{\rm sat})\Re\sum_{m<n}e^{i\boldsymbol{Q}(\boldsymbol{R}_m-\boldsymbol{R}_n)}\frac{2i\Delta_n}{(4\Delta_m^2+2I_{\rm p}/I_{\rm sat})(4\Delta_n^2+2I_{\rm p}/I_{\rm sat})} \tag{55}$$

$$-e^{-2W}2(I_{\rm p}/I_{\rm sat})\Re\sum_{m<n}e^{i\boldsymbol{Q}(\boldsymbol{R}_m-\boldsymbol{R}_n)}\frac{2i\Delta_m}{(4\Delta_m^2+2I_{\rm p}/I_{\rm sat})(4\Delta_n^2+2I_{\rm p}/I_{\rm sat})} \tag{56}$$

$$e^{-2W}2(I_{\rm p}/I_{\rm sat})\Re\sum_{m<n}e^{i\boldsymbol{Q}(\boldsymbol{R}_m-\boldsymbol{R}_n)}\frac{1}{(4\Delta_m^2+2I_{\rm p}/I_{\rm sat})(4\Delta_n^2+2I_{\rm p}/I_{\rm sat})} \tag{57}$$

Furthermore, if we detune the light in between the two spin states then we can use, $\Delta_m^2=\Delta^2$ and $\Delta_m = 2|\Delta|S_{zm}$, where $S_{zm}=\pm\frac{1}{2}$ is the spin state of the atom in site m, to obtain

$$e^{-2W}2(I_{\rm p}/I_{\rm sat})\frac{16\Delta^2}{(4\Delta^2+2I_{\rm p}/I_{\rm sat})^2}\Re\sum_{m<n}e^{i\boldsymbol{Q}(\boldsymbol{R}_m-\boldsymbol{R}_n)}S_{zm}S_{zn} \tag{58}$$

$$e^{-2W}2(I_{\rm p}/I_{\rm sat})\frac{4i|\Delta|}{(4\Delta^2+2I_{\rm p}/I_{\rm sat})^2}\Re\sum_{m<n}e^{i\boldsymbol{Q}(\boldsymbol{R}_m-\boldsymbol{R}_n)}S_{zn} \tag{59}$$

$$-e^{-2W}2(I_{\rm p}/I_{\rm sat})\frac{4i|\Delta|}{(4\Delta^2+2I_{\rm p}/I_{\rm sat})^2}\Re\sum_{m<n}e^{i\boldsymbol{Q}(\boldsymbol{R}_m-\boldsymbol{R}_n)}S_{zm} \tag{60}$$

$$e^{-2W}2(I_{\rm p}/I_{\rm sat})\frac{1}{(4\Delta^2+2I_{\rm p}/I_{\rm sat})^2}\Re\sum_{m<n}e^{i\boldsymbol{Q}(\boldsymbol{R}_m-\boldsymbol{R}_n)} \tag{61}$$

We identify the first term and the last term as related to the spin structure factor and crystal structure factor. In this last equation we see that the first term, the one related to the spin structure factor, is going to have the main contribution to the intensity because it goes as $|\Delta|^{-2}$, whereas the other terms

go as larger powers of $1/|\Delta|$. If we neglect terms other than the first one, we obtain

$$\begin{aligned} I &= \left(\frac{\hbar c k \Gamma}{r_D^2}\frac{9}{24\pi}\Lambda\right)\left[e^{-2W}\frac{16\Delta^2(I_\mathrm{p}/I_\mathrm{sat})}{(4\Delta^2+2I_\mathrm{p}/I_\mathrm{sat})^2}2\Re\sum_{m<n}e^{i\boldsymbol{Q}(\boldsymbol{R}_m-\boldsymbol{R}_n)}S_{zm}S_{zn}+\sum_n\frac{1}{2}\frac{2I_\mathrm{p}/I_\mathrm{sat}}{4\Delta^2+2I_\mathrm{p}/I_\mathrm{sat}}\right] \\ &= \left(\frac{\hbar c k \Gamma}{r_D^2}\frac{9}{24\pi}\Lambda\right)\frac{I_\mathrm{p}/I_\mathrm{sat}}{4\Delta^2+2I_\mathrm{p}/I_\mathrm{sat}}\left[\frac{e^{-2W}16\Delta^2}{(4\Delta^2+2I_\mathrm{p}/I_\mathrm{sat})}2\Re\sum_{m<n}e^{i\boldsymbol{Q}(\boldsymbol{R}_m-\boldsymbol{R}_n)}S_{zm}S_{zn}+N\right] \end{aligned} \tag{62}$$

For the first sum, exchanging indexes in the summand results in its complex conjugate, so it can be replaced using $2\Re\sum_{m<n}\equiv\sum_{m\neq n}$. We also use $\sum_{m\neq n}\equiv\sum_{mn}-\sum_{m=n}$ to obtain

$$\begin{aligned} I &= \left(\frac{\hbar c k \Gamma}{r_D^2}\frac{9}{24\pi}\Lambda\right)\frac{I_\mathrm{p}/I_\mathrm{sat}}{4\Delta^2+2I_\mathrm{p}/I_\mathrm{sat}}\left[\frac{e^{-2W}16\Delta^2}{(4\Delta^2+2I_\mathrm{p}/I_\mathrm{sat})}\left(\sum_{mn}-\sum_{m=n}\right)e^{i\boldsymbol{Q}(\boldsymbol{R}_m-\boldsymbol{R}_n)}S_{zm}S_{zn}+N\right] \\ &= \left(\frac{\hbar c k \Gamma}{r_D^2}\frac{9}{24\pi}\Lambda\right)\frac{I_\mathrm{p}/I_\mathrm{sat}}{4\Delta^2+2I_\mathrm{p}/I_\mathrm{sat}}\left[\frac{e^{-2W}4\Delta^2}{(4\Delta^2+2I_\mathrm{p}/I_\mathrm{sat})}\left(4\sum_{mn}e^{i\boldsymbol{Q}(\boldsymbol{R}_m-\boldsymbol{R}_n)}S_{zm}S_{zn}-N\right)+N\right] \end{aligned} \tag{63}$$

We consider a measurement of the intensity after a large time-of-flight (TOF), denoted as $I_{\boldsymbol{Q}\infty}$. After TOF, the Debye-Waller factor goes to zero due to the expanding size of the atomic wavefunction, so we have

$$I_{\boldsymbol{Q}\infty} = \left(\frac{\hbar c k \Gamma}{r_D^2}\frac{9}{24\pi}\Lambda\right)\frac{I_\mathrm{p}/I_\mathrm{sat}}{4\Delta^2+2I_\mathrm{p}/I_\mathrm{sat}}N \tag{64}$$

and therefore

$$\frac{I_{\boldsymbol{Q}}}{I_{\boldsymbol{Q}\infty}} = \frac{e^{-2W}4\Delta^2}{(4\Delta^2+2I_\mathrm{p}/I_\mathrm{sat})}\left(\frac{4}{N}\sum_{mn}e^{i\boldsymbol{Q}(\boldsymbol{R}_m-\boldsymbol{R}_n)}S_{zm}S_{zn}-1\right)+1 \tag{65}$$

2 Measurement of the structure factor

The theorists in our collaboration calculate the spin structure factor, S, for a given value of the momentum transfer $\boldsymbol{Q}$. The spin structure factor is defined as

$$S_{\boldsymbol{Q}} = \frac{4}{N}\sum_{mn}e^{i\boldsymbol{Q}(\boldsymbol{R}_m-\boldsymbol{R}_n)}S_{zm}S_{zn} \tag{66}$$

From inspection of Eq. 65 we see that a measurement of $I_{\boldsymbol{Q}}/I_{\boldsymbol{Q}\infty}$ can be related to the spin structure factor by

$$\frac{I_{\boldsymbol{Q}}}{I_{\boldsymbol{Q}\infty}} = \frac{e^{-2W}4\Delta^2}{(4\Delta^2+2I_\mathrm{p}/I_\mathrm{sat})}\left(S_{\boldsymbol{Q}}-1\right)+1 \tag{67}$$

At this point we introduce the notation

$$\frac{I_{\boldsymbol{Q}}}{I_{\boldsymbol{Q}\infty}} \equiv i_{\boldsymbol{Q}} \qquad\qquad c \equiv \frac{e^{-2W}4\Delta^2}{(4\Delta^2+2I_\mathrm{p}/I_\mathrm{sat})} \tag{68}$$

to obtain

$$i_{\boldsymbol{Q}} = c(S_{\boldsymbol{Q}}-1)+1 \tag{69}$$

For a measurement in a deep enough lattice ($e^{-2W} \to 1$) and with a low intensity probe ($I_\mathrm{p}/I_\mathrm{sat} \ll 2\Delta^2$) the TOF normalized intensity and the structure factor are equivalent:

$$i_{\boldsymbol{Q}} = S_{\boldsymbol{Q}} \tag{70}$$

In our experiment we are using $I_\mathrm{p}/I_\mathrm{sat} \approx 15$ and $\Delta = 6.5$. We perform the measurement at a lattice depth of $50E_R$. For these parameters we have the following:

$$\begin{aligned} e^{-2W} &= 0.81 \\ 1 + \frac{I_\mathrm{p}/I_\mathrm{sat}}{2\Delta^2} &= 1.18 \end{aligned} \tag{71}$$

$$S_{\boldsymbol{Q}} - 1 = 1.45 \times (i_{\boldsymbol{Q}} - 1) \tag{72}$$

2.1 Magneto-association and contributions from doubly occupied sites

In our experiment we have the possibility to magneto-associate (MA) the atoms in doubly occupied sites prior to a measurement of the scattered light. The formed molecules are largely detuned from the probe light and the light that they scatter is negligible. In this section we study the implications of MA for the comparison between experimental measurements and the structure factor as calculated by the theorists.

We start from Eq. 63 and will separate the sums over atoms in singly and doubly occupied sites. Without carrying out the sums, Eq. 63 reads

$$I_{\boldsymbol{Q}} = \frac{I_{\boldsymbol{Q}\infty}}{N}\left[4c\sum_{mn} e^{i\boldsymbol{Q}(\boldsymbol{R}_m - \boldsymbol{R}_n)} S_{zm} S_{zn} - c\sum_n + \sum_n\right] \tag{73}$$

With MA prior to the intensity measurement, there is no contribution to the scattered light from atoms in doubly occupied sites, so denoting as $\mathcal{S}$ the set of singly occupied sites, we have

$$\begin{aligned} I_{\boldsymbol{Q}_\mathrm{MA}} &= \frac{I_{\boldsymbol{Q}\infty}}{N}\left[4c\sum_{m\in\mathcal{S}} e^{i\boldsymbol{Q}\boldsymbol{R}_m} S_{zm} \sum_{n\in\mathcal{S}} e^{-i\boldsymbol{Q}\boldsymbol{R}_n} S_{zn} - c\sum_{n\in\mathcal{S}} + \sum_{n\in\mathcal{S}}\right] \\ &= \frac{I_{\boldsymbol{Q}\infty}}{N}\left[4c\sum_{m\in\mathcal{S}} e^{i\boldsymbol{Q}\boldsymbol{R}_m} S_{zm} \sum_{n\in\mathcal{S}} e^{-i\boldsymbol{Q}\boldsymbol{R}_n} S_{zn} - cN(1-D) + N(1-D)\right] \end{aligned} \tag{74}$$

where D is the fraction of atoms in doubly occupied sites.

Denoting the set of atoms in doubly occupied sites as $\mathcal{D}$, we point out that

$$\sum_{m\in\mathcal{D}} e^{\pm i\boldsymbol{Q}\boldsymbol{R}_m} S_{zm} = 0 \tag{75}$$

since the contributions cancel out in pairs as $e^{\pm i\boldsymbol{Q}\boldsymbol{R}_m}(+1/2 - 1/2) = 0$. This allows us to remove the $\in \mathcal{S}$ constraint in the remaining sums:

$$\sum_{m\in\mathcal{S}} e^{\pm i\boldsymbol{Q}\boldsymbol{R}_m} S_{zm} = \sum_m e^{\pm i\boldsymbol{Q}\boldsymbol{R}_m} S_{zm} \tag{76}$$

and obtain for the intensity after MA

$$\begin{aligned} I_{\boldsymbol{Q}_{\mathrm{MA}}} &= \frac{I_{\boldsymbol{Q}\infty}}{N}\left[4c\sum_m e^{i\boldsymbol{Q}\boldsymbol{R}_m}S_{zm}\sum_n e^{-i\boldsymbol{Q}\boldsymbol{R}_n}S_{zn} - cN(1-D) + N(1-D)\right] \\ &= I_{\boldsymbol{Q}\infty}\left[cS_{\boldsymbol{Q}} - c(1-D) + (1-D)\right] \end{aligned} \tag{77}$$

We introduce the simplifying notation

$$\frac{I_{\boldsymbol{Q}_{\mathrm{MA}}}}{I_{\boldsymbol{Q}\infty}} \equiv i_{\boldsymbol{Q}_{\mathrm{MA}}} \tag{78}$$

and solve for the spin structure factor to obtain

$$S_{\boldsymbol{Q}} = \frac{1}{c}\left(i_{\boldsymbol{Q}_{\mathrm{MA}}} - 1\right) + 1 + \frac{D}{c}(1-c) \tag{79}$$

To measure the fraction of atoms in doubly occupied sites, D, we can make a measurement of the scattered intensity after MA and a large TOF. Combined with the TOF measurement without MA we have

$$D = 1 - \frac{I_{\boldsymbol{Q}_{\mathrm{MA}\infty}}}{I_{\boldsymbol{Q}\infty}} \equiv 1 - i_S \tag{80}$$

giving finally

$$S_{\boldsymbol{Q}} = \frac{i_{\boldsymbol{Q}_{\mathrm{MA}}}}{c} + \frac{c-1}{c}i_S \tag{81}$$

We have taken sets of data where we only record $I_{\boldsymbol{Q}_{\mathrm{MA}\infty}}$ and $I_{\boldsymbol{Q}_{\mathrm{MA}}}$. Under this conditions we can use the following two equations to solve for the structure factor

$$\frac{I_{\boldsymbol{Q}_{\mathrm{MA}}}}{I_{\boldsymbol{Q}\infty}} = cS_{\boldsymbol{Q}} - c(1-D) + (1-D) \qquad \frac{I_{\boldsymbol{Q}_{\mathrm{MA}\infty}}}{I_{\boldsymbol{Q}\infty}} = 1 - D \tag{82}$$

$$S_{\boldsymbol{Q}} = \frac{1-D}{c}(j_{\boldsymbol{Q}_{\mathrm{MA}}} + c - 1) \qquad j_{\boldsymbol{Q}_{\mathrm{MA}}} \equiv \frac{I_{\boldsymbol{Q}_{\mathrm{MA}}}}{I_{\boldsymbol{Q}_{\mathrm{MA}\infty}}} \tag{83}$$

We still need knowledge of the double occupancy D, so for sets with only $I_{\boldsymbol{Q}_{\mathrm{MA}\infty}}$ and $I_{\boldsymbol{Q}_{\mathrm{MA}}}$ we have to use D from another data set.

2.2 Data at short time-of-flight

In the above section we considered $I_{\boldsymbol{Q}\infty}$, a measurement of the intensity with a time-of-flight long enough such that the Debye-Waller factor $e^{-2W} \to 0$. For some of the data we have taken, the TOF is 6 μs, which in some cases is not long enough for the Debye-Waller factor be negligible. In this section we look at the determination of $S_{\boldsymbol{Q}}$ with time of flight data for which one cannot assume $e^{-2W} \to 0$.

We recall that the Debye-Waller factor is defined as

$$e^{-2W} = \prod_{i=x,y,z} e^{-Q_i^2\langle r_i^2\rangle} \tag{84}$$

where Q_i is the i^{th} component of the momentum transfer $\boldsymbol{Q} = \boldsymbol{k}' - \boldsymbol{k}$, with $\boldsymbol{k}'$ and $\boldsymbol{k}$ the wave vectors of the outgoing and incoming light respectively. The time-of-flight dependence of the Debye-Waller factor is through the expanding size of the atomic wavefunctions. For an in-situ picture $\langle r_i^2\rangle$ corresponds to the position spread of the lattice site's harmonic oscillator ground state. After the atoms are released

from the lattice the spread of the wavefunction satisfies

$$\begin{aligned}\langle r_i^2\rangle_t =&\langle r_i^2\rangle_0 + \frac{t^2}{m^2}\langle p_i^2\rangle_0 \\ =&\langle r_i^2\rangle_0 + \frac{t^2}{m^2}\frac{\hbar^2}{4\langle r_i^2\rangle_0}\end{aligned} \tag{85}$$

In a harmonic oscillator potential we have

$$\langle r^2\rangle = \frac{\hbar}{2m\omega} \tag{86}$$

and since in a lattice of depth V_0 recoils, $\hbar\omega = 2E_R\sqrt{V_0}$

$$\langle r^2\rangle = \frac{a^2}{2\pi^2\sqrt{V_0}} \tag{87}$$

where a is the lattice spacing.

We then have for the Debye-Waller factor as a function of time-of-flight

$$\begin{aligned}[e^{-2W}]_t =& \prod_{i=x,y,z}\exp\left[-Q_i^2\left(\frac{a^2}{2\pi^2\sqrt{V_0}} + \frac{h^2\sqrt{V_0}}{8a^2}\frac{t^2}{m^2}\right)\right] \\ =&[e^{-2W}]_0\prod_{i=x,y,z}\exp\left[-Q_i^2\frac{h^2\sqrt{V_0}}{8a^2}\frac{t^2}{m^2}\right] \\ =&[e^{-2W}]_0\prod_{i=x,y,z}\exp\left[-\frac{\sqrt{V_0}}{2}\left(\frac{Q_i h}{2ma}\right)^2 t^2\right] \\ =&[e^{-2W}]_0\exp\left[-\frac{\sqrt{V_0}}{2}\left(\frac{|\boldsymbol{Q}|h}{2ma}\right)^2 t^2\right]\end{aligned} \tag{88}$$

We now define the time dependent correction factor

$$c(t) = \frac{[e^{-2W}]_t 4\Delta^2}{4\Delta^2 + 2I_{\rm p}/I_{\rm sat}} \tag{89}$$

The measured intensity after time-of-flight t is

$$\frac{I_{\boldsymbol{Q}}(t)}{I_{\boldsymbol{Q}\infty}} = c(t)(S_{\boldsymbol{Q}} - 1) + 1 \tag{90}$$

Consider two measurements, one at $t = 0$, the other one at $t = T$,

$$\frac{I_{\boldsymbol{Q}}(t=0)}{I_{\boldsymbol{Q}\infty}} = c(0)(S_{\boldsymbol{Q}} - 1) + 1 \qquad \frac{I_{\boldsymbol{Q}}(t=T)}{I_{\boldsymbol{Q}\infty}} = c(T)(S_{\boldsymbol{Q}} - 1) + 1 \tag{91}$$

Their ratio is

$$\frac{I_{\boldsymbol{Q}}(t=0)}{I_{\boldsymbol{Q}}(t=T)} = \frac{c(0)(S_{\boldsymbol{Q}} - 1) + 1}{c(T)(S_{\boldsymbol{Q}} - 1) + 1} \equiv i_{\boldsymbol{Q}_T} \tag{92}$$

which can be solved to give

$$S_{\boldsymbol{Q}} = \frac{1 - c(0) - i_{\boldsymbol{Q}_T}(1 - c(T))}{i_{\boldsymbol{Q}_T}c(T) - c(0)} \tag{93}$$

2.3 Simultaneous measurement of the structure factor for two different values of $\boldsymbol{Q}$

In the sections above we have shown how to measure the spin structure factor $S_{\boldsymbol{Q}}$ by measuring the scattered intensity in-situ and after time-of-flight. An issue that arises with this measurement is that the in-situ and TOF measurements require two different realizations of the experiment.

In our setup we have the possibility of measuring the scattered intensity at two different output angles. One of the angles corresponds to a momentum transfer $\boldsymbol{Q} = \frac{2\pi}{a}(\frac{1}{2}\ \frac{1}{2}\ \frac{1}{2}) \equiv \boldsymbol{\pi}$, which offers the possibility of measuring the staggered magnetization of the system, i.e. the degree of antiferromagnetic ordering. The other angle corresponds to a momentum transfer $\boldsymbol{Q} = \frac{2\pi}{a}(0.4,\ -0.1,\ -0.04) \equiv \boldsymbol{\theta}$. The structure factor can also be measured at this value of $\boldsymbol{Q}$ and compared with theoretical calculations. Since this momentum transfer does not measure the staggered magnetization it may be used as a normalization for the measurement at $\boldsymbol{Q} = \boldsymbol{\pi}$

For the measurements at $\boldsymbol{\pi}$ and $\boldsymbol{\theta}$ we have (without magneto-association)

$$S_{\boldsymbol{\pi}} = (i_{\boldsymbol{\pi}} - 1 + c_{\boldsymbol{\pi}})/c_{\boldsymbol{\pi}} \qquad S_{\boldsymbol{\theta}} = (i_{\boldsymbol{\theta}} - 1 + c_{\boldsymbol{\theta}})/c_{\boldsymbol{\theta}} \tag{94}$$

$$\frac{S_{\boldsymbol{\pi}}}{S_{\boldsymbol{\theta}}} = \frac{i_{\boldsymbol{\pi}} - 1 + c_{\boldsymbol{\pi}}}{i_{\boldsymbol{\theta}} - 1 + c_{\boldsymbol{\theta}}} \left(\frac{c_{\boldsymbol{\theta}}}{c_{\boldsymbol{\pi}}}\right) \tag{95}$$

To make use of the simultaneous measurement of I at $\boldsymbol{Q} = \boldsymbol{\pi}, \boldsymbol{\theta}$ we define

$$\left(\frac{I_{\boldsymbol{\pi}}}{I_{\boldsymbol{\theta}}}\right) \Big/ \left(\frac{I_{\boldsymbol{\pi}\infty}}{I_{\boldsymbol{\theta}\infty}}\right) \equiv i_{\boldsymbol{\pi}/\boldsymbol{\theta}} \tag{96}$$

The advantage here is that the ratio $\frac{I_{\boldsymbol{\pi}\infty}}{I_{\boldsymbol{\theta}\infty}}$ is determined only by the solid angle and responsivity of the cameras. One can calibrate this ratio beforehand and then, using the calibration, get a single shot measurement of $i_{\boldsymbol{\pi}/\boldsymbol{\theta}}$

The ratio of the structure factors at $\boldsymbol{\pi}$ and $\boldsymbol{\theta}$ is given by

$$\frac{S_{\boldsymbol{\pi}}}{S_{\boldsymbol{\theta}}} = \frac{i_{\boldsymbol{\pi}/\boldsymbol{\theta}} - (1 - c_{\boldsymbol{\pi}})/i_{\boldsymbol{\theta}}}{1 - (1 - c_{\boldsymbol{\theta}})/i_{\boldsymbol{\theta}}} \left(\frac{c_{\boldsymbol{\theta}}}{c_{\boldsymbol{\pi}}}\right) \tag{97}$$

If our correction factors were close to 1 we could obtain the ratio of structure factors in one shot as

$$\frac{S_{\boldsymbol{\pi}}}{S_{\boldsymbol{\theta}}} \approx i_{\boldsymbol{\pi}/\boldsymbol{\theta}} \tag{98}$$

Besides being able to get this in one shot it has the added advantage that any common mode noise between the two cameras gets canceled out, this includes atom number fluctuations and fluctuations in the intensity or polarization of the probe light. Unfortunately with our $50\,E_R$ lattice and $I_{\mathrm{p}}/I_{\mathrm{sat}} = 15$ we have

$$c_{\boldsymbol{\pi}} = 0.686 \qquad c_{\boldsymbol{\theta}} = 0.805 \tag{99}$$

which results in a non-negligible correction that depend on $i_{\boldsymbol{\theta}}$. In our case this is not such a drawback because the camera located at $\boldsymbol{\theta}$ has a solid angle that is 10 time larger than the camera located at $\boldsymbol{\pi}$.

We can also obtain formulas for the ratio $S_{\boldsymbol{\pi}}/S_{\boldsymbol{\theta}}$ under the conditions described in the two previous sections.

In the case where the time-of-flight is not large enough for $e^{-2W} \to 0$ we have the formula

$$\frac{S_{\boldsymbol{\pi}}}{S_{\boldsymbol{\theta}}} = \frac{[1 - c_{\boldsymbol{\pi}}(0)]/i_{\boldsymbol{\theta}_T} - i_{(\boldsymbol{\pi}/\boldsymbol{\theta})_T}[1 - c_{\boldsymbol{\pi}}(T)]}{[1 - c_{\boldsymbol{\theta}}(0)]/i_{\boldsymbol{\theta}_T} - [1 - c_{\boldsymbol{\theta}}(T)]} \frac{c_{\boldsymbol{\theta}}(T) - c_{\boldsymbol{\theta}}(0)/i_{\boldsymbol{\theta}_T}}{i_{(\boldsymbol{\pi}/\boldsymbol{\theta})_T} c_{\boldsymbol{\pi}}(T) - c_{\boldsymbol{\pi}}(0)/i_{\boldsymbol{\theta}_T}} \tag{100}$$

If the in-situ intensity is measured after magneto-association we have

$$\frac{S_{\boldsymbol{\pi}}}{S_{\boldsymbol{\theta}}} = \frac{c_{\boldsymbol{\theta}}}{c_{\boldsymbol{\pi}}} \frac{i_{(\boldsymbol{\pi}/\boldsymbol{\theta})_{\mathrm{MA}}} + (c_{\boldsymbol{\pi}} - 1)(1 - D)/i_{\boldsymbol{\theta}_{\mathrm{MA}}}}{1 + (c_{\boldsymbol{\theta}} - 1)(1 - D)/i_{\boldsymbol{\theta}_{\mathrm{MA}}}} \tag{101}$$

If both the in-situ and TOF intensity are measured after magneto-association we have

$$\frac{S_{\boldsymbol{\pi}}}{S_{\boldsymbol{\theta}}} = \frac{c_{\boldsymbol{\theta}}}{c_{\boldsymbol{\pi}}} \frac{j_{(\boldsymbol{\pi}/\boldsymbol{\theta})_{\mathrm{MA}}} + (c_{\boldsymbol{\pi}} - 1)/j_{\boldsymbol{\theta}_{\mathrm{MA}}}}{1 + (c_{\boldsymbol{\theta}} - 1) j_{\boldsymbol{\theta}_{\mathrm{MA}}}} \tag{102}$$

2.4 Summary of structure factor formulas

Below we show the different ways to calculate the structure factor from our measurements. A correction factor, $c_{\boldsymbol{Q}}$ appears in the formulas to account for the non-unity Debye-Waller factor in the lattice and also for the intensity of the probe beam. The formula for the correction factor is

$$c_{\boldsymbol{Q}} = \frac{e^{-2W} 4\Delta^2}{(4\Delta^2 + 2I_\mathrm{p}/I_\mathrm{sat})} \tag{103}$$

The Debye-Waller factor, e^{-2W} depends on the momentum transfer $\boldsymbol{Q}$. In our experiment the corrections are significant. The largest lattice depth we can reach is $50\,E_R$, and in order to moderately overcome the dark noise of the camera we use a probe intensity of $I_p = 15\,I_\mathrm{sat}$. This results in the following values for $\boldsymbol{\pi}$ and $\boldsymbol{\theta}$, the two values of the momentum transfer that we have access to:

$$\boldsymbol{\pi} = \frac{2\pi}{a}(0.5,\, 0.5,\, 0.5) \qquad \boldsymbol{\theta} = \frac{2\pi}{a}(0.4,\, -0.1,\, -0.04) \tag{104}$$

$$e_{\boldsymbol{\pi}}^{-2W} = 0.81 \qquad e_{\boldsymbol{\theta}}^{-2W} = 0.95 \qquad 1 + \frac{I_\mathrm{p}/I_\mathrm{sat}}{2\Delta^2} = 1.18 \tag{105}$$

$$c_{\boldsymbol{\pi}} = 0.686 \qquad c_{\boldsymbol{\theta}} = 0.805 \tag{106}$$

The duration of our scattering pulse is $1.7\,\mu$s, and we scatter on the average 4.7 photons per atom. At our lattice depth of $50\,E_R$, the square of the Lamb-Dicke parameter is $\eta_{LD}^2 = 0.07$ which means that we can approximately scatter 14 photons per atom before we kick the atom into an excited band. At the moment we have not introduced corrections for atoms recoiling into excited bands during the measurement.

In the latest data that we have taken at $5.5\,E_R$ as a function of U/t, we always do a magneto-association sweep before the in-situ picture. We also take time-of-flight pictures with and without magneto-association. The following table lists the quantities that we measure

CCD measurements:

$I_{\boldsymbol{Q}_\mathrm{MA}}$	In-situ intensity measured at momentum transfer $\boldsymbol{Q}$ after magneto-association of doubly occupied sites into molecules. Molecules are dark to the probe light.
$I_{\boldsymbol{Q}\infty}$	Time-of-flight intensity measured at momentum transfer $\boldsymbol{Q}$. We use TOF = $10\,\mu$s.
$I_{\boldsymbol{Q}_{\mathrm{MA}\infty}}$	Time-of-flight intensity measured at momentum transfer $\boldsymbol{Q}$ after magneto-association of doubly occupied sites into molecules. Molecules are dark to the probe light.

Ratios of CCD measurements:

$i_{\boldsymbol{Q}_{\rm MA}}$	$\frac{I_{\boldsymbol{Q}_{\rm MA}}}{I_{\boldsymbol{Q}\infty}}$ For a given U/t the set of $I_{\boldsymbol{Q}_{\rm MA}}$ is averaged and the set of $I_{\boldsymbol{Q}\infty}$ is averaged, then the ratio is calculated.
i_S	$\frac{I_{\boldsymbol{Q}_{\rm MA}\infty}}{I_{\boldsymbol{Q}\infty}} \equiv 1-D$, where D is the double occupancy. For a given U/t the set of $I_{\boldsymbol{Q}_{\rm MA}\infty}$ is averaged and the set of $I_{\boldsymbol{Q}\infty}$ is averaged, then the ratio is calculated.
$i_{(\boldsymbol{\pi}/\boldsymbol{\theta})_{\rm MA}}$	$\left(\frac{I_{\boldsymbol{\pi}_{\rm MA}}}{I_{\boldsymbol{\theta}_{\rm MA}}}\right)\Big/\left(\frac{I_{\boldsymbol{\pi}\infty}}{I_{\boldsymbol{\theta}\infty}}\right)$ For a given U/t the set of $\frac{I_{\boldsymbol{\pi}_{\rm MA}}}{I_{\boldsymbol{\theta}_{\rm MA}}}$ is averaged and the set of $\frac{I_{\boldsymbol{\pi}\infty}}{I_{\boldsymbol{\theta}\infty}}$ is averaged, then the ratio is calculated.
$f_{(\boldsymbol{\pi}/\boldsymbol{\theta})_{\rm MA}}$	$\left(\frac{I_{\boldsymbol{\pi}_{\rm MA}}}{I_{\boldsymbol{\theta}_{\rm MA}}}\right)\Big/\overline{\left(\frac{I_{\boldsymbol{\pi}\infty}}{I_{\boldsymbol{\theta}\infty}}\right)}$ For a given U/t the set of $\frac{I_{\boldsymbol{\pi}_{\rm MA}}}{I_{\boldsymbol{\theta}_{\rm MA}}}$ is averaged. The set of $\frac{I_{\boldsymbol{\pi}\infty}}{I_{\boldsymbol{\theta}\infty}}$ is averaged for all data at any U/t value. This can be done since the TOF ratio depends only on the solid angle and the responsivity of the CCDs.

We the use the quantities in the table above to determine the two structure factors and their ratio in the following ways:

Structure factor formulas relevant for latest data

0.	$S_{\boldsymbol{\pi}}/S_{\boldsymbol{\theta}}$	$\frac{c_{\boldsymbol{\theta}}}{c_{\boldsymbol{\pi}}}\frac{i_{(\boldsymbol{\pi}/\boldsymbol{\theta})_{\rm MA}}+(c_{\boldsymbol{\pi}}-1)(1-D)/i_{\boldsymbol{\theta}_{\rm MA}}}{1+(c_{\boldsymbol{\theta}}-1)(1-D)/i_{\boldsymbol{\theta}_{\rm MA}}}$	$i_{(\boldsymbol{\pi}/\boldsymbol{\theta})_{\rm MA}}$ is used.
1.	$S_{\boldsymbol{\theta}}$	$\frac{i_{\boldsymbol{\theta}_{\rm MA}}}{c_{\boldsymbol{\theta}}}+\frac{c_{\boldsymbol{\theta}}-1}{c_{\boldsymbol{\theta}}}(1-D)$	For the determination of D we use $D=1-i_S$
2.	$S_{\boldsymbol{\pi}}$	$\frac{i_{\boldsymbol{\pi}_{\rm MA}}}{c_{\boldsymbol{\pi}}}+\frac{c_{\boldsymbol{\pi}}-1}{c_{\boldsymbol{\pi}}}(1-D)$	For the determination of D we use $D=1-i_S$
3.	$S_{\boldsymbol{\pi}}/S_{\boldsymbol{\theta}}$	$\frac{c_{\boldsymbol{\theta}}}{c_{\boldsymbol{\pi}}}\frac{f_{(\boldsymbol{\pi}/\boldsymbol{\theta})_{\rm MA}}+(c_{\boldsymbol{\pi}}-1)(1-D)/i_{\boldsymbol{\theta}_{\rm MA}}}{1+(c_{\boldsymbol{\theta}}-1)(1-D)/i_{\boldsymbol{\theta}_{\rm MA}}}$	$f_{(\boldsymbol{\pi}/\boldsymbol{\theta})_{\rm MA}}$ is used. This means that we use the calibration of the ratio of the two cameras, which leads to an improvement in the signal to noise ratio because common mode noise between the two cameras cancels out.
5.	$S_{\boldsymbol{\pi}}$	$\frac{S_\pi}{S_\theta}S_\theta$	The results of 1. and 3. are combined to obtain $S_{\boldsymbol{\pi}}$.

In the data plot shown below each panel has a number on the top left corner indicating which formula is used to obtain the data.

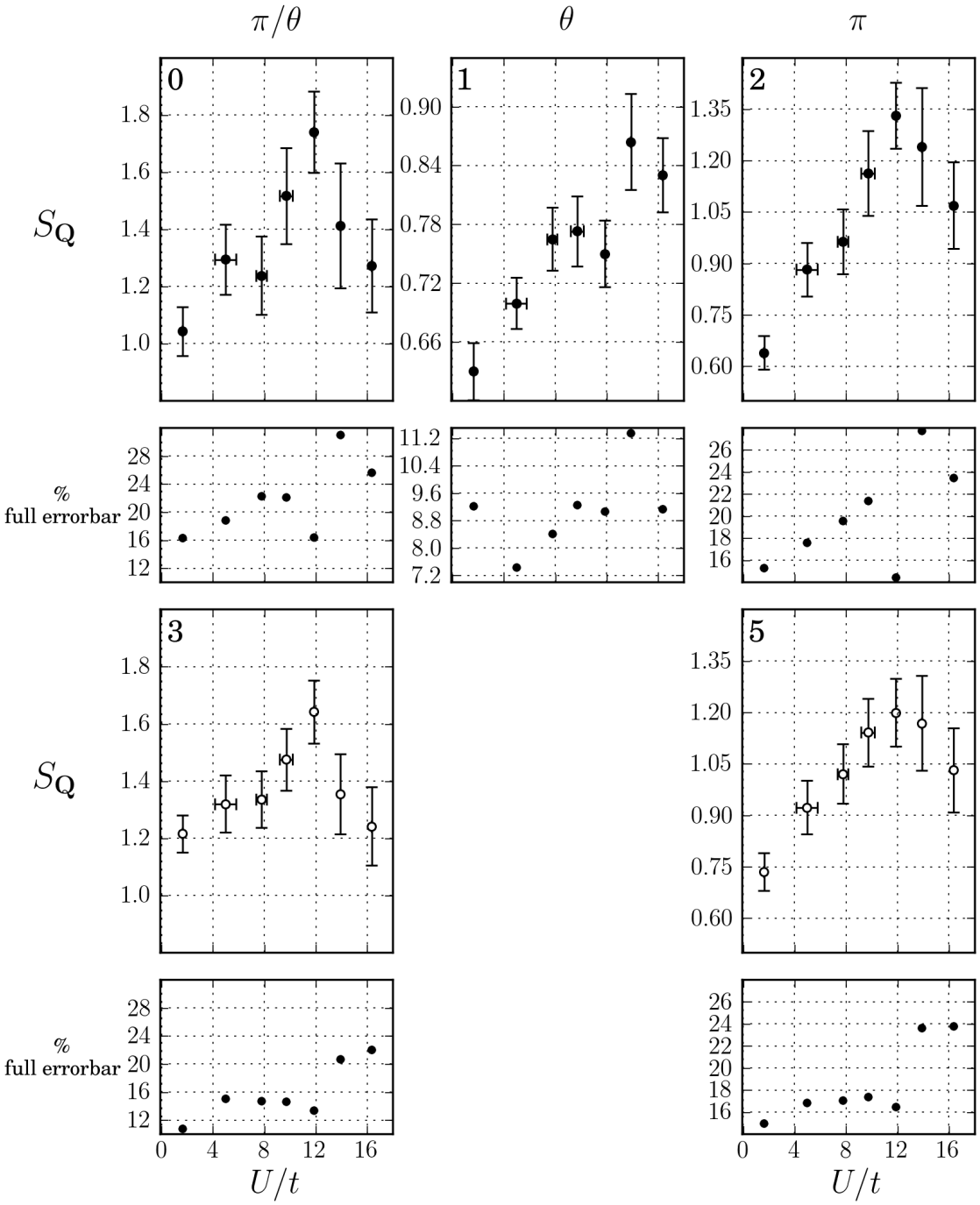

2.5 Comments

The first row and the third row of the plot shown above involve two different ways to get to the structure factor from our data. They are pretty close to each other within error bars but not fully consistent. We think that the most direct way to get to $S_{\boldsymbol{\pi}}$ is in the first row. The most direct way to get to the ratio $S_{\boldsymbol{\pi}}/S_{\boldsymbol{\theta}}$ is in the third row, since it uses the calibrated ratio $f_{(\boldsymbol{\pi}/\boldsymbol{\theta})_{\mathrm{MA}}}$ which only depends on the solid angle and responsivity of the cameras.

3 Sample inhomogeneity

The Quantum Monte Carlo (QMC) calculations done by the theorists in our collaboration are for systems with uniform filling, and at a fixed value of the interaction strength U/t. Our sample is far from these uniform conditions. Since it is a trapped finite sample, the filling (density) goes all the way down to zero. Typically, optical lattices are realized with laser beams that have large beam waists, so the parameters U and t have a negligible variation over the size of the sample. In our experiment we used a beam waist ($\approx 45\,\mu$m) which is comparable to the size of the sample ($1/e$ radius of $\approx 20\,\mu$m). For this reason we have a strong variation of U and t over the size of the sample. In our system, as you move from the center to the outside of the atom cloud the lattice gets shallower, which results in reduced U and increased t. The Hubbard interaction strength U/t thus suffers from both numerator and denominator which results in a significant variation of U/t over the cloud.

The motivation for reducing U and increasing t in length scales comparable with the sample is such that there may be entropy redistribution to the edges of the cloud. Near the edges the system has a larger entropy capacity due to the lower filling there. Additionally, since towards the edge the lattice is shallower, elastic collisions may lead to evaporation of the particles which may resulting in cooling of the system.

To incorporate the effects of inhomogeneity in the comparison between QMC and our measurements we will divide our sample into five bins, each with equal number of particles and then get the values of the filling n and of U/t for each of the bins. QMC calculations of the structure factor can be performed for each bin and then averaged before comparing with the experimental results.

To calculate the average value of n and U/t in each bin we need knowledge of the density profile of our cloud, as well as knowledge of our optical lattice potential. The potential can be calculated from the calibrated beam waists and power of our optical lattice beams.

For the density profile we can perform in-situ phase-contrast images of the atom cloud. Alternatively, with our known atom number and the calculated potential we can use a thermodynamic model of the system to calculate the expected density distribution. The thermodynamic model we use is the high temperature series expansion up to second order in T/t, which can be calculated readily and is accurate down to about $T/t \approx 1.8$. To avoid complications with the repeatability in the realization of a certain density distribution we choose this second alternative. We feed into the model the atom number measured in the experiment. As a sanity check we can plot a particular realization of the density distribution and compare it with the calculation from the thermodynamic model. We can check if the peak density, double occupancy, and cloud size roughly agree with the model.

In Fig. 1 we show a plot of the in-situ density distribution measured using phase-contrast imaging in a $5.5\,E_R$ lattice with $3.0\,E_R$ of green compensation. It can be seen that the distribution is not spherically symmetric and that the atoms are pushed to the left of the picture. The $1/e$ sizes are 15.1 μm and 23.8 μm. The number of atoms in the cloud is 360,000. The density at the peak is estimated from the number and the cloud sizes to be 6.53e12 cm^{-3} which corresponds to 0.98 atoms per site. The image shown was taken at a scattering length of 326 a_0.

If we put 360,000 atoms into the model we obtain the results shown in Fig. 2 for various values of the green compensation. The peak density and double occupancy depend sensitively on the green compensation. In order to calculate the density profiles that will be used to estimate the effect of inhomogeneity on the spin structure factor we have to pick a value for the green compensation. The value that we use in the experiment is $3\,E_R$, but our observations of the peak density and the double occupancy as a function of scattering length do not match the model at $3\,E_R$ compensation. Our measurement of the double occupancy in the $5.5\,E_R$ lattice is shown in Fig. 3 and it resembles the curve with a compensation of $2.6\,E_R$ in the model (the x axis in both plots is in different units but the points

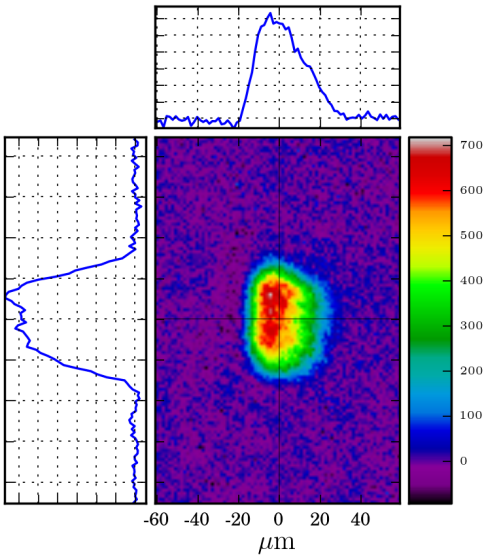

Figure 1: In-situ density distribution in a $5.5\,E_R$ lattice with $3\,E_R$ of green compensation.

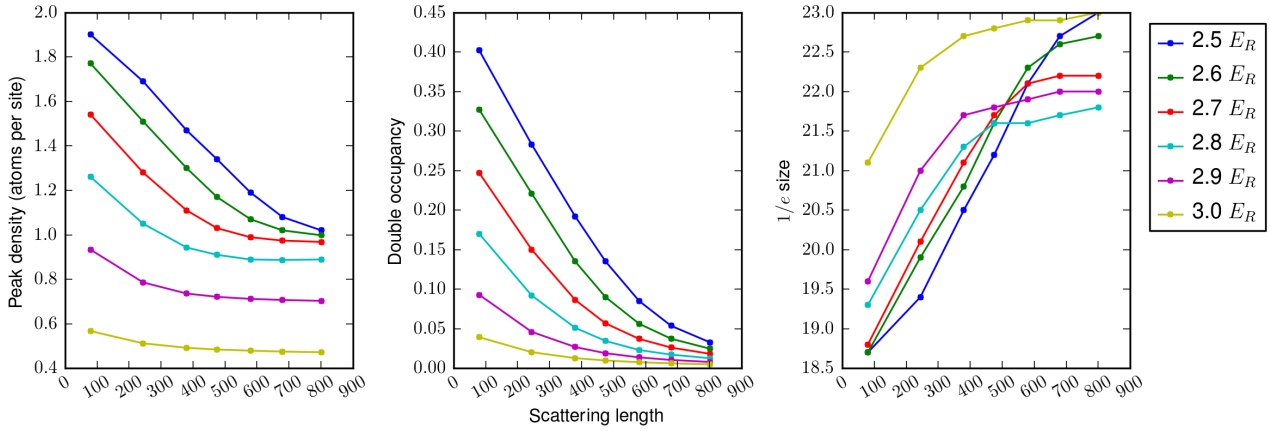

Figure 2: System parameters as a function of scattering length for various values of the green compensation. The model used is the high temperature series expansion.

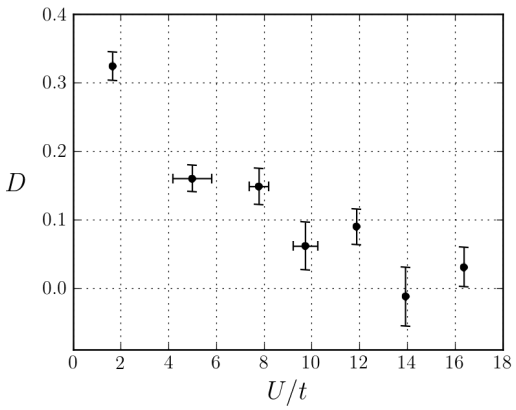

Figure 3: Double occupancy in the $5.5\,E_R$ lattice.

shown correspond between the two plots). Our measurement of the density at 326 a_0 is more consistent with a compensation of $2.8\,E_R$ in the model. The discrepancy between our measurements and the model is most likely due to calibration errors and our inexact knowledge of the potential, however since the temperature used for the model is $T/t = 1.8$ it is possible that the discrepancy is also due to a lower temperature in our system than the one this model can handle. In what follows we will use $2.7\,E_R$ in the model to split the difference between the peak density and double occupancy observation and stay somewhat consistent with our observations.

With all the parameters that go into the model in hand, we can go ahead and calculate density distributions. We then split those density distributions into bins with an equal number of atoms and calculate the average filling and U/t for each bin. An example of this calculation for a scattering length of 580 a_0, which corresponds to $[U/t]_0 = 11.9$ is shown in Fig. 4. $[U/t]_0$ stands for U/t at the center, which is the value that we have been using as the x axis in all our structure factor plots so far.

Below we proceed to tabulate the binned filling and U/t for the values of $[U/t]_0$ that correspond to the data that we have taken in the $5.5\,E_R$ lattice

[U/t]_0 = 1.636		
bin#	n	U/t
000	1.24	1.43
001	0.85	1.17
002	0.50	0.95
003	0.16	0.68
004	0.02	0.29

[U/t]_0 = 4.976		
bin#	n	U/t
000	1.04	4.26
001	0.71	3.41
002	0.43	2.75
003	0.14	1.92
004	0.02	0.78

[U/t]_0 = 7.771		
bin#	n	U/t
000	0.93	6.56
001	0.65	5.19
002	0.39	4.12
003	0.12	2.78
004	0.02	1.08

[U/t]_0 = 9.713		
bin#	n	U/t
000	0.89	8.19
001	0.63	6.41
002	0.37	5.01
003	0.11	3.36
004	0.01	1.30

[U/t]_0 = 11.86		
bin#	n	U/t
000	0.86	9.89
001	0.61	7.75
002	0.37	6.12
003	0.12	4.10
004	0.01	1.58

[U/t]_0 = 13.905		
bin#	n	U/t
000	0.85	11.60
001	0.59	8.98
002	0.36	7.07
003	0.12	4.76
004	0.01	1.78

[U/t]_0 = 16.359		
bin#	n	U/t
000	0.84	13.66
001	0.59	10.57
002	0.36	8.32
003	0.12	5.60
004	0.01	2.10

To make matters simpler, and since this treatment is only a crude estimation we create a single table averaging the seven tables above, such that we obtain values for the filling and percentage of $[U/t]_0$ for

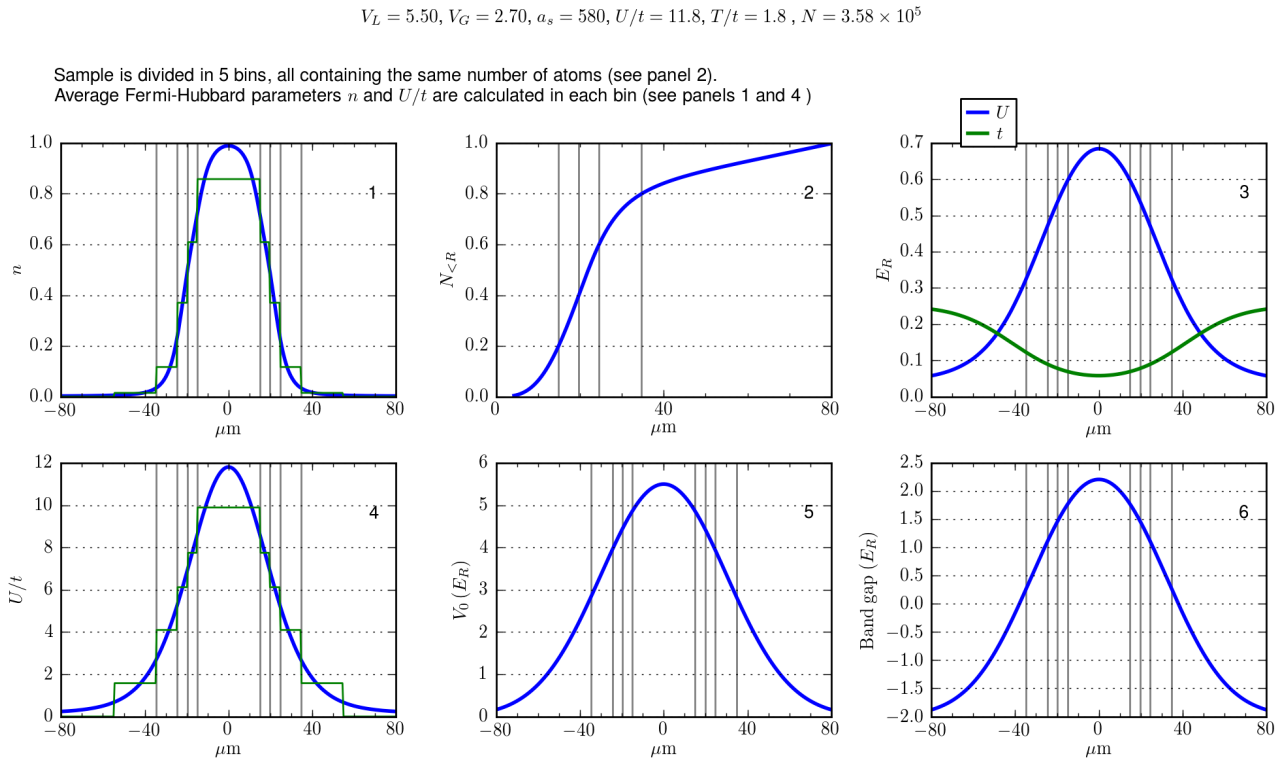

Figure 4: Binned filling and U/t are shown in the left column, panels 1 and 4. The average value in each bin is shown in green. The cumulative number up to a certain radius is shown in panel 2, this illustrates how all the bins have the same number of atoms. The radial dependence of other relevant parameters are shown in panels 3, 5, and 6.

a general case. This table is what we suggest should be used to estimate the effect of inhomogeneity of our sample on the structure factor. The column labeled n denotes the fillings for each of the five bins, and the last seven columns denote the value of U/t in each of the five bins for the seven values of $[U/t]_0$ that we have in our data.

bin#	n	%U/t	1.6	5.0	7.8	9.7	11.9	13.9	16.4
000	0.95	85	1.4	4.2	6.6	8.2	10.0	11.8	13.8
001	0.66	67	1.1	3.3	5.2	6.5	7.9	9.3	10.9
002	0.40	53	0.9	2.6	4.1	5.2	6.3	7.4	8.7
003	0.13	36	0.6	1.8	2.8	3.5	4.3	5.0	5.9
004	0.02	14	0.2	0.7	1.1	1.4	1.7	2.0	2.3

3.1 Raw data for S_π/S_θ and S_π

Below we show the raw data for the best estimate of S_π/S_θ which uses the simultaneous measurement of both cameras with a calibrated normalization. This is panel 3 on the figure with the data.

U/t	Spi/Sth	error
1.6	1.21	0.065
5.0	1.32	0.099
7.8	1.34	0.098
9.7	1.48	0.108
11.9	1.64	0.110
13.9	1.35	0.140
16.4	1.24	0.136

Below we show $S_{\boldsymbol{\pi}}$ determined from $S_{\boldsymbol{\pi}}/S_{\boldsymbol{\theta}}$ and $S_{\boldsymbol{\theta}}$, this is panel 5 on the figure with the data .

U/t	Spi	error
1.6	0.735	0.055
5.0	0.923	0.078
7.8	1.021	0.087
9.7	1.141	0.099
11.9	1.199	0.099
13.9	1.168	0.138
16.4	1.031	0.123

Below we show $S_{\boldsymbol{\pi}}$ determined using only the camera at $\boldsymbol{\pi}$, this is panel 2 on the figure with the data.

U/t	Spi	error
1.6	0.639	0.049
5.0	0.882	0.078
7.8	0.963	0.094
9.7	1.162	0.124
11.9	1.331	0.096
13.9	1.240	0.172
16.4	1.069	0.125

References

[1] R. Loudon, *The Quantum Theory of Light*, *Oxford Science Publications* (OUP Oxford, 2000).

[2] C. Cohen-Tannoudji, J. Dupont-Roc, and G. Grynberg, *Atom-Photon Interactions: Basic Processes and Applications*, *A Wiley-Interscience publication* (Wiley, 1998).